



Performance improvement of anode-supported electrolytes for planar solid oxide fuel cells via a tape-casting/lamination/co-firing technique

Hae-Gu Park^a, Hwan Moon^a, Sung-Chul Park^a, Jong-Jin Lee^a, Daeil Yoon^a, Sang-Hoon Hyun^{a,*}, Do-Heyoung Kim^b

^a School of Advanced Materials Science and Engineering, Yonsei University, Seoul 120-749, Republic of Korea

^b Research Institute of Industrial Science and Technology, Kyungpook 790-600, Republic of Korea

ARTICLE INFO

Article history:

Received 11 August 2009

Received in revised form 8 October 2009

Accepted 16 November 2009

Available online 26 November 2009

Keywords:

Solid oxide fuel cell

Flatness

Tape-casting/lamination/co-firing

Warp

Power output

ABSTRACT

Recently, solid oxide fuel cells (SOFCs) have attracted considerable attention because of their low emissions, high-energy conversion efficiency, and flexible usage of various fuels. One of the key problems of applying flat-type SOFCs to large-scale power generation is that unit cells of large area and with a high degree of flatness cannot be manufactured satisfactorily.

In this study, the effects of tape-casting, laminating, and co-firing conditions on the flatness of anode-supported electrolyte unit cells have been investigated to improve the cell performance of unit cells. The cells are composed of a Ni-yttria-stabilized zirconia (YSZ) anode, a Ni-YSZ anode functional layer (AFL), a YSZ electrolyte, and a lanthanum strontium manganate (LSM)-YSZ cathode. The flatness of the anode-supported electrolyte is optimized by controlling the firing schedule, the lamination method, and the applied load during firing. A 5 cm × 5 cm (active area 4 cm × 4 cm) unit cell having a reasonable flatness of 55 μm/5 cm shows a higher power output of 11.4 W as compared with 7.7 W a unit cell with a flatness of 200 μm/5 cm, when operating at 800 °C with humidified hydrogen fuel.

© 2009 Elsevier B.V. All rights reserved.

1. Introduction

Solid oxide fuel cells (SOFCs) have been developed for next-generation power systems because of their high efficiencies and use of diverse fuel sources. In particular, a planar-type design is widely chosen for SOFCs because of its low fabrication cost and high power density [1,2]. To commercialize planar SOFCs, a cost-effective process for manufacturing anode-supported unit cells of a larger size and higher performance is needed. Among the various techniques [3–7], the tape-casting/lamination/co-firing (TLC) process would be the most suitable for producing anode-supported electrolytes because the process is used in the mass production of tapes. In addition, co-firing of electrodes and electrolyte layers is also a low-cost means of manufacturing SOFCs, and its successful application would decrease energy consumption by reducing the number of heat-treatment steps.

In this study, single cells with an anode-supported electrolyte are fabricated by the TLC technique. It should be noted, however,

that controlling the flatness of large-sized unit cells prepared by the TLC technique is known to be a challenge because of mismatches between the thermo-mechanical and physical properties of the individual layers [8]. The anode-supported electrolyte is warped due to the mismatch between the thermal expansion coefficient (TEC) of the yttria-stabilized zirconia (YSZ) and that of NiO-YSZ cermet. The TEC of the YSZ electrolyte is $10.2\text{--}10.8 \times 10^{-6} \text{ K}^{-1}$, whereas that of the NiO-YSZ cermet is $13.0\text{--}13.4 \times 10^{-6} \text{ K}^{-1}$.

The flatness of the planar unit cell is crucial to the performance of planar SOFCs because a flatter cell offers a greater contact area for the current-collectors. The flatness of a cell is considerably dependent on the warp phenomena, which can easily occur during the burn-out and sintering processes. Therefore, the interrelationships between the flatness, warping and cell performance of the anode-supported unit cells prepared by the TLC technique require thorough investigation to improve the performance and durability of SOFCs.

To fabricate planar SOFC unit cells cost-effectively by the TLC technique, the present research has focused on the following topics: (1) improvement in the flatness of anode-supported electrolytes via control of the warp phenomena during the burn-out and sintering phases, and control of the warp effect on unit cell performance, and (2) evaluation of the effects of the flatness of the anode-supported electrolyte in improving performance of the unit cells.

* Corresponding author at: School of Advanced Materials Science and Engineering, Yonsei University, 2nd Eng. Building, Rm B420, 134 Shinchon-dong, Seodaemun-gu, Seoul, 120-749, Republic of Korea. Tel.: +82 2 2123 2850; fax: +82 2 365 5882.

E-mail addresses: prohsh@yonsei.ac.kr, cprocess@yonsei.ac.kr (S.-H. Hyun).

Table 1
Compositions of anode, NiO–YSZ AFL, NiO/YSZ–YSZ AFL and YSZ electrolyte slurry for tape-casting.

Component	Powder (wt.%)				Solvent (wt.%)		Dispersant (wt.%)	Binder solution (wt.%)
	NiO (J.T. Baker)	NiO/YSZ–YSZ nanocomposite powder	YSZ TZ-8Y (Tosoh)	YSZ (FYT FYT13.0-010H (Unitec ceramics))	Carbon black Raven 430 (Columbian chemical)	Toluene (Dongyang)		
Anode	22.7	-	9.0	9.0	4.5	27.5	6.9	19.5
	Ni:YSZ vol. ratio = 4:6	-	7.0	7.0	4.5	27.5	6.9	19.5
	Ni:YSZ vol. ratio = 5:5	-	5.3	5.3	4.5	27.5	6.9	19.5
	Ni:YSZ vol. ratio = 6:4	-	19.9	-	-	27.5	6.9	19.5
NiO–YSZ AFL	25.3	-	5	-	-	27.5	6.9	19.5
NiO/YSZ–YSZ AFL	6.3	33.9	5	-	-	27.5	6.9	19.5
YSZ electrolyte	-	-	49	-	-	24.5	6.1	19.6

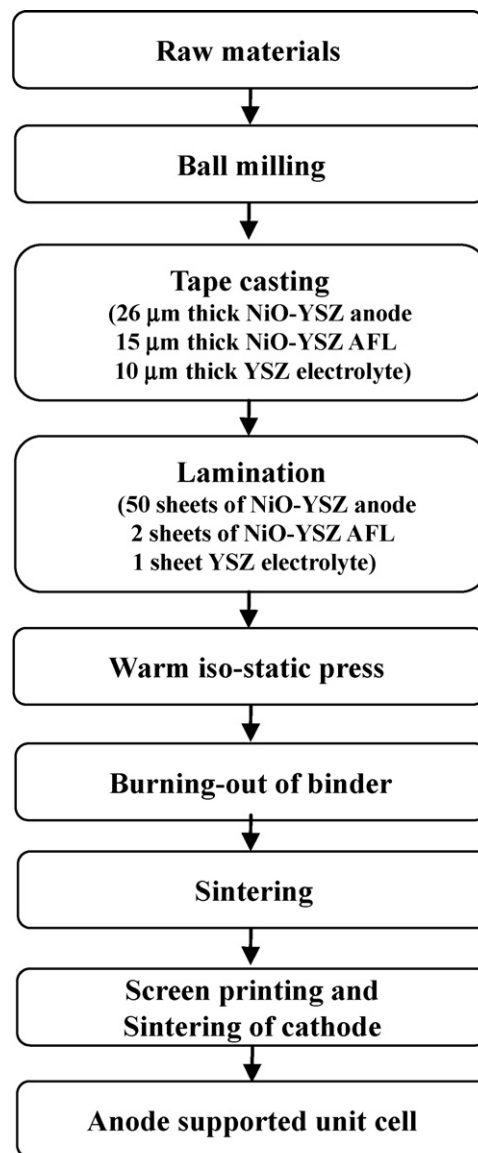


Fig. 1. Flow chart of manufacturing procedure for anode-supported electrolyte via TLC technique.

2. Experimental procedure

2.1. Fabrication of anode-supported electrolyte

Commercial powders of NiO (Nickelous oxide green, J.T. Baker, USA), fine YSZ (TZ-8Y, TOSOH, Japan), coarse YSZ (FYT13.0-010H, Unitec Ceramics, UK), NiO/YSZ–YSZ nanocomposite [11] and carbon black (Raven 430, Columbian Chemical, USA) were used as raw materials to prepare the NiO–YSZ anode, the NiO/YSZ anode functional layer (AFL), the NiO/YSZ–YSZ AFL, and the YSZ electrolyte. The slurry compositions of the NiO–YSZ anode, the NiO–YSZ AFL, the NiO/YSZ–YSZ AFL and the YSZ electrolyte for tape-casting are given in Table 1. The procedure for manufacturing the anode-supported cell by means of the TLC technique is shown in Fig. 1.

The raw materials were first mixed and ball-milled in solvents (toluene and ethanol) with a dispersant for 24 h, and then ball-milled again with a commercial binder solution for 24 h to form a homogeneous slurry. Tape-casting was performed using a tape-caster (Hansung system, Korea), by which slurry was coated on a polyethylene (PET) carrier film at a rate of 2 cm s^{-1} at 70°C . The

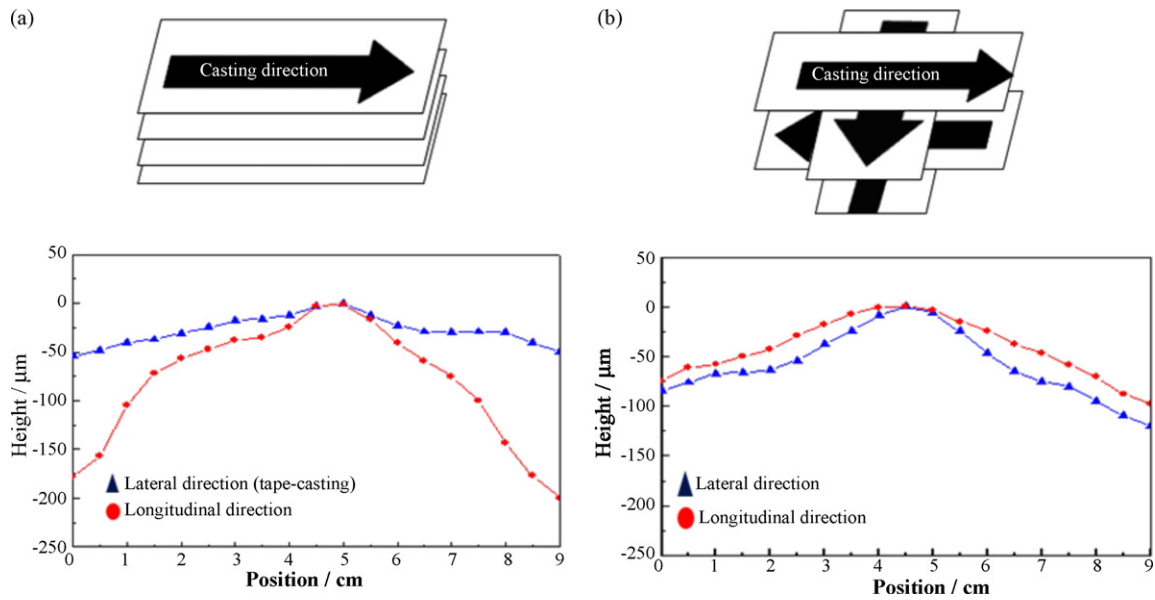


Fig. 2. Schematic of lamination method and flatness of anode-supported electrolyte depending on lamination method: (a) one-directional laminating process and (b) four-directional laminating process.

thicknesses of the green tapes so produced were $26\ \mu\text{m}$ for the anode, $15\ \mu\text{m}$ for the AFL, and $10\ \mu\text{m}$ for the electrolyte. After sintering, the thicknesses of the electrolyte tapes were 20, 10 and $8\ \mu\text{m}$, respectively. The anode-supported electrolytes were laminated with 50 anode sheets, two AFL sheets, and one electrolyte sheet. An AFL tape was laminated between the electrolyte tape and the anode tapes. To improve the performance of the cell, an AFL composed of NiO/YSZ-YSZ was prepared. The specimens ($10\ \text{cm} \times 10\ \text{cm}$ tape size) were laminated by means of a four-directional method for relaxation of the residual internal stress of the tapes. After the laminating steps, the specimens were pressed iso-statically at $3500\ \text{N cm}^{-2}$ and $70\ ^\circ\text{C}$ for 15 min to improve both strength and flatness. The specimens were then cut into $9\ \text{cm} \times 9\ \text{cm}$ sizes.

2.2. Heat-treatment of anode-supported electrolyte

The burn-out and sintering conditions were subjected to heat-treatment at $1100\ ^\circ\text{C}$ for 3 h and at $1350\ ^\circ\text{C}$ for 3 h, respectively [10]. Several heat-treatments at the burn-out conditions were executed to effect adequate decomposition of the polymer additives.

The heating and cooling rates for the sintering conditions were set at $5\ ^\circ\text{C min}^{-1}$. The morphology of the anode-supported electrolyte was observed with a scanning electron microscope (SEM S4200, Hitachi, Japan).

The warpage behaviour of the anode-supported electrolyte during burn-out without loading was captured with a digital camera (COOLPIX 4100, Nikon, Japan) every 20 min [12]. In addition, the warpage behaviour of the laminate during sintering without loading was monitored with a video recorder (HDR-SR-7, Sony, Japan).

The shrinkage rate ($\Delta L/L_0$) was measured by the change in length of the NiO-YSZ anode, the NiO-YSZ AFL, and the YSZ electrolyte samples ($5\ \text{mm} \times 5\ \text{mm} \times 2\ \text{mm}$) during the burn-out and sintering. The shrinkage characteristics were observed using a dilatometer (DIL402C, Netzsch, Germany) in an air atmosphere. To improve the flatness of the anode-supported electrolyte, the electrolytes were loaded diversely with a porous zirconia setter during the burn-out and sintering. In this study, the flatness is defined as the camber of the longitude and latitude from the centre of the specimens. The flatness of the sintered sample was measured by an indicator (543-250, MITUTOYO, Japan) every $0.5\ \text{cm}$.

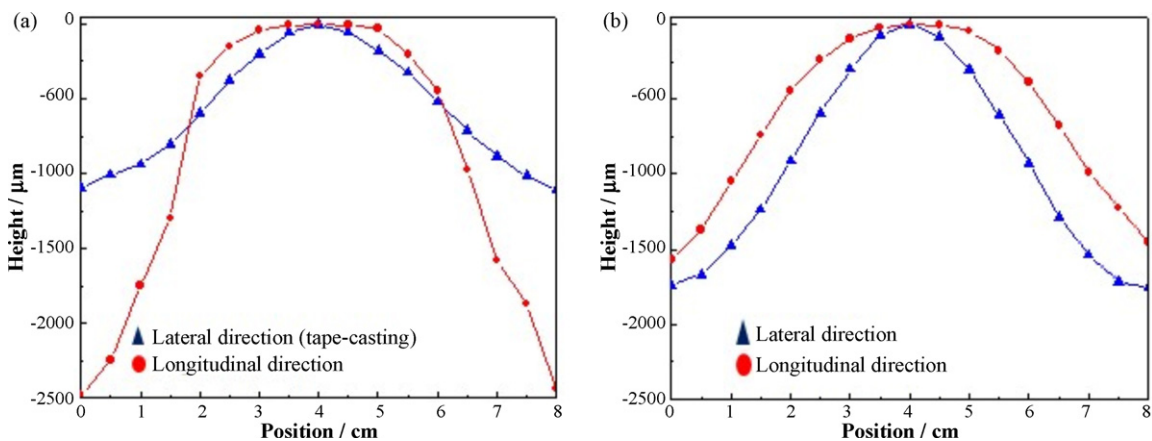


Fig. 3. Flatness of anode-supported electrolyte depending on lamination method after burn-out of binder: (a) one-directional laminating process and (b) four-directional laminating process.

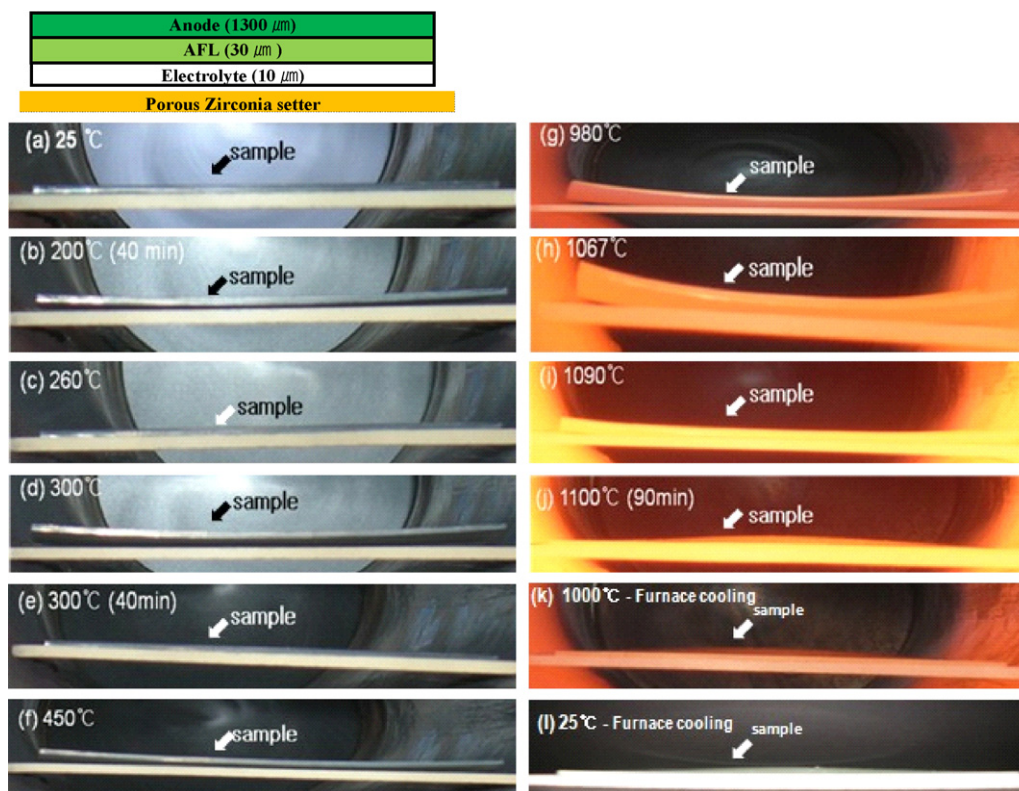


Fig. 4. Schematic of anode-supported electrolyte and behaviour of anode-supported electrolyte during burn-out. *Time indicated by round brackets is dwelling time.

2.3. Performance tests

The cathode paste was prepared using in-house $\text{La}_{0.8}\text{Sr}_{0.2}\text{MnO}_3$ (LSM20-P, Fuel Cell Materials, USA)-YSZ (TZ-8Y) with a weight ratio of 50:50. The performance of the in-house LSM-YSZ cathode was fixed to concentrate on the effects of the developed anode-supported electrolytes. The cathode layer was screen-printed on the anode-supported electrolyte with an active area of $4\text{ cm} \times 4\text{ cm}$ and a thickness of $50\text{ }\mu\text{m}$. The cathode layer was sintered at $1150\text{ }^\circ\text{C}$ for 3 h. Single-cell performances were evaluated at $800\text{ }^\circ\text{C}$ in reactive gases of humidified hydrogen (400 cc min^{-1}) with 3% H_2O and air (600 cc min^{-1}) current-voltage I - V characterization of the $5\text{ cm} \times 5\text{ cm}$ anode-supported cell was undertaken.

3. Results and discussion

3.1. Optimization of flatness of the anode-supported electrolyte

In this type of experiment, the optimization of the slurry composition is a very important procedure because the final microstructures of the specimens are strongly dependent on their green microstructures. In our previous investigations [9,10], the anode, commercial AFL and electrolyte layer were cast homogeneously.

The anode-supported electrolyte was fabricated by the anode tape to have a $26\text{-}\mu\text{m}$ green thickness, an AFL tape with a $15\text{-}\mu\text{m}$ green thickness, and an electrolyte with a $10\text{-}\mu\text{m}$ green thickness. The laminate was composed of 50 sheets of anode, 2 sheets of AFL, and 1 sheet of electrolyte.

The lamination method is a very important step to produce a flat anode-supported electrolyte because the thickness deviation of the anode tape is about $3\text{--}4\text{ }\mu\text{m}$. Two lamination methods were performed to determine the optimum lamination method. The first method was a one-directional laminating process that laminated

repeatedly in the casting direction only. The second method was a four-directional process that laminated with repeated 90-degree clockwise turns.

After laminating the tapes, the samples were pressed isostatically at 3500 N cm^{-2} and $70\text{ }^\circ\text{C}$ for 15 min to improve the strength and flatness. Then, the samples were cut to $9\text{ cm} \times 9\text{ cm}$ and their flatness measured by an indicator. The centre of the anode was set to zero. The camber of the longitude and latitude from the centre of the specimen was measured every 0.5 cm . The lamination method has an effect on the flatness of the laminates. The flatness of the laminates made by the first and second method is $200\text{ }\mu\text{m}/9\text{ cm}$ and $120\text{ }\mu\text{m}/9\text{ cm}$, respectively (Fig. 2). The flatness of the laminate is improved with the relaxation mechanism of the residual internal stress in tapes using the four-directional method.

Binder organics and carbon black are completely removed during the 3 h burn-out at $1100\text{ }^\circ\text{C}$. After burn-out, the laminate size is decreased to 8.6 cm with a small amount of warp. Fig. 3 illustrates the flatness of the sample after warm iso-static pressing of the sample after burn-out. The flatness of the laminates produced using the first method and the second method is $2500\text{ }\mu\text{m}/8\text{ cm}$ and $1750\text{ }\mu\text{m}/8\text{ cm}$, respectively.

The warp evolution of the anode-supported electrolyte during burn-out is presented in Fig. 4. The YSZ electrolyte of the laminate is in contact with the porous zirconia setter because the carbon black of the anode is effectively burnt-out. The time indicated by the round brackets is the dwelling time. The sample is put on the zirconia setter at $25\text{ }^\circ\text{C}$ and warps continuously up to $200\text{ }^\circ\text{C}$ for 40 min. The sample flattens continuously until $260\text{ }^\circ\text{C}$. The sample warps continuously from $300\text{ }^\circ\text{C}$ (40 min) to $1067\text{ }^\circ\text{C}$. The sample quickly flattens at $1067\text{ }^\circ\text{C}$. The centre of the sample rises markedly at $1100\text{ }^\circ\text{C}$ (90 min). The shape does not change from $1100\text{ }^\circ\text{C}$ (90 min) to $25\text{ }^\circ\text{C}$. The laminate appears to warp and flatten repeatedly during burn-out. Also, the warping direction is always toward the anode (convex warping). Fig. 5 shows that the shrinkage rate of

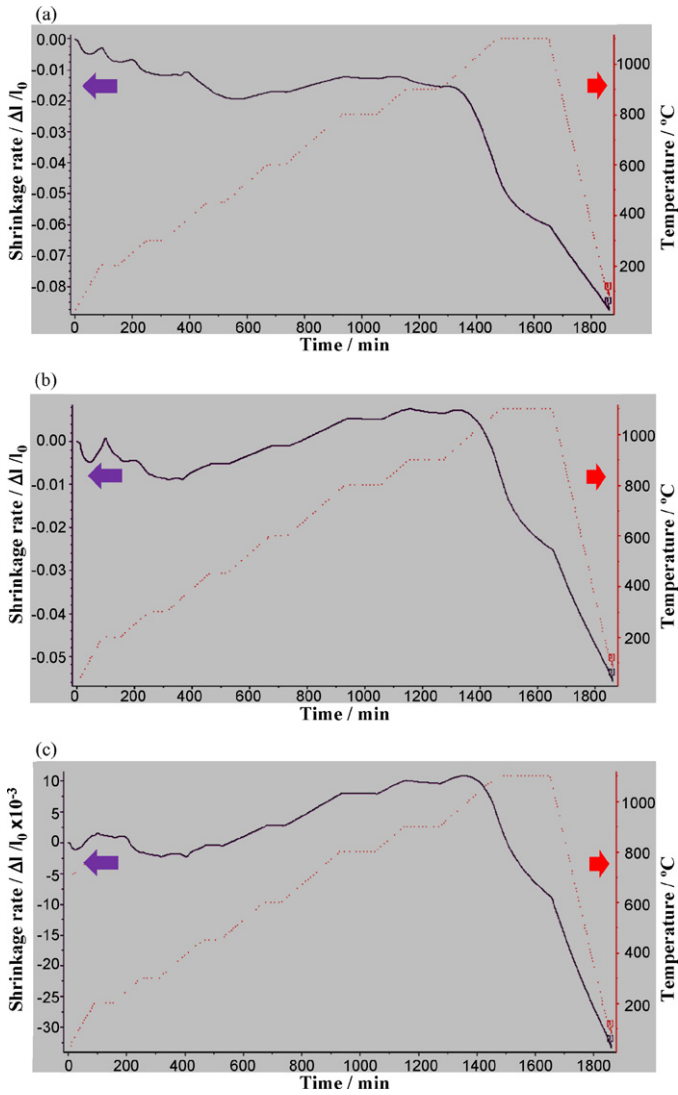


Fig. 5. Shrinkage rates of each component during burn-out: (a) anode, (b) AFL, and (c) electrolyte.

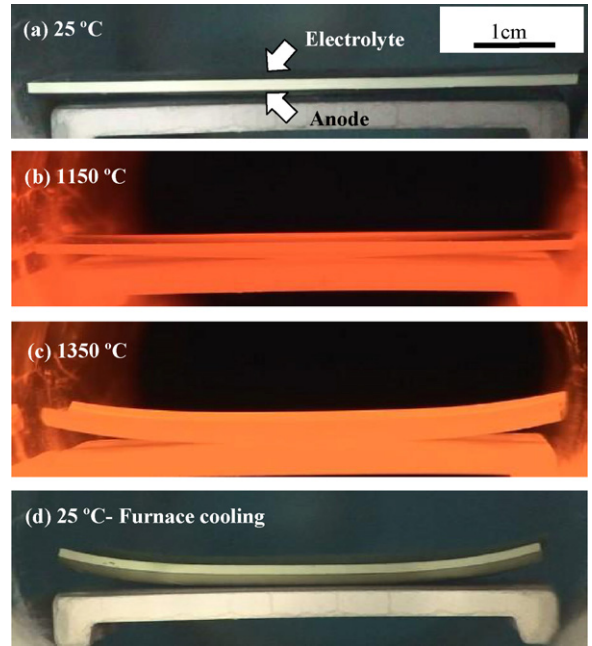


Fig. 7. Behaviour of anode-supported electrolyte during sintering.

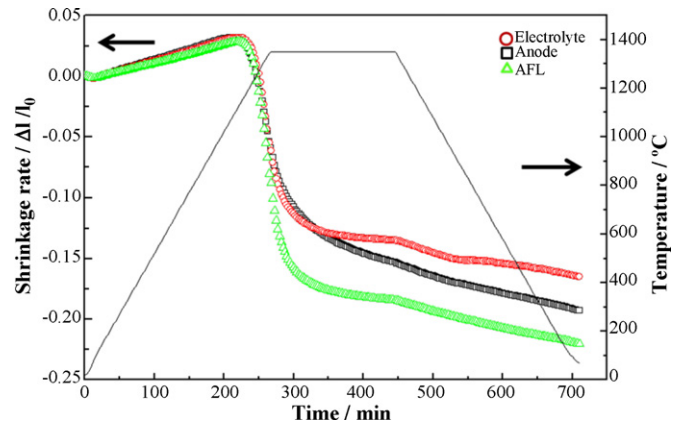


Fig. 8. Shrinkage rates of each component during sintering: (a) anode, (b) AFL, and (c) electrolyte.

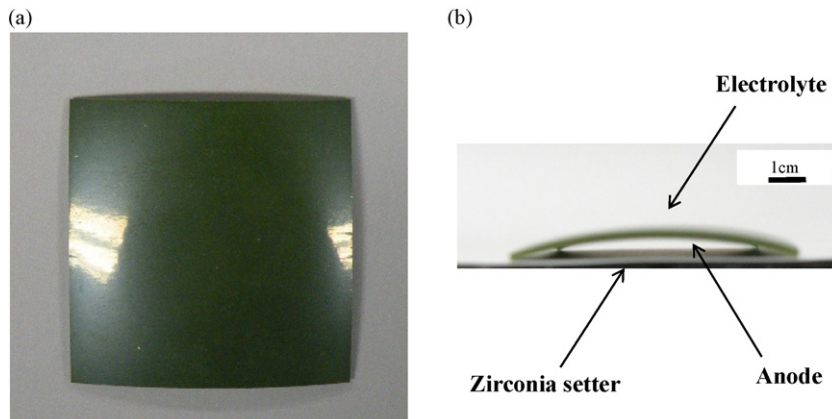


Fig. 6. Warpage of sintered anode-supported electrolyte: (a) top view and (b) side view.

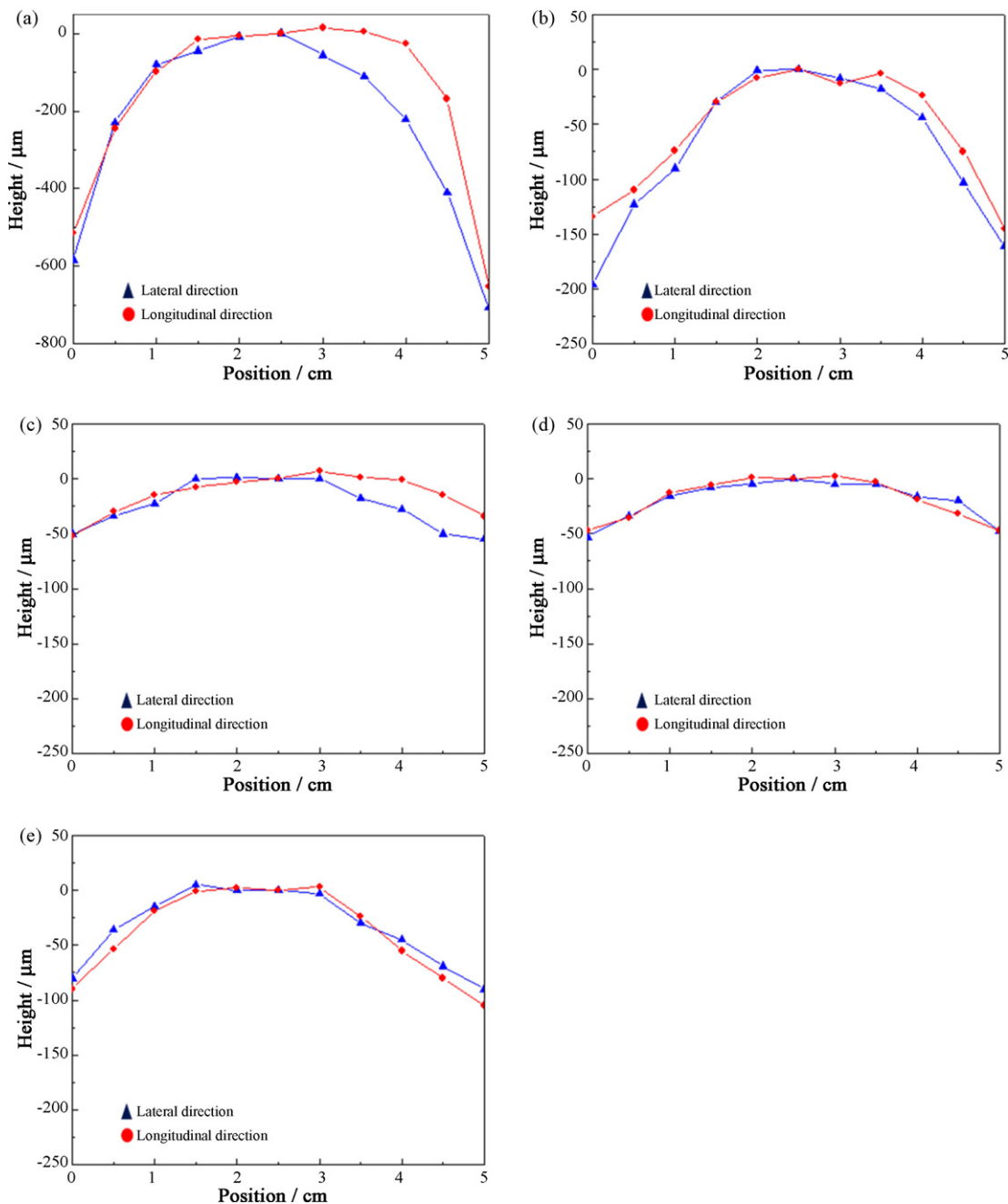


Fig. 9. Flatness of anode-supported electrolyte depending on applied load: (a) 0 Pa, (b) 460.6 Pa, (c) 597.8 Pa, (d) 1107.4 Pa, and (e) 1793.4 Pa.

the anode (a) is larger than those of the AFL (b) and the YSZ electrolyte (c) because the carbon black of the anode is removed during burn-out. The AFL matches between the anode and the electrolyte. The shrinkage stress of the anode and electrolyte is decreased by inserting the AFL. Bao et al. [13] suggested that a model of the anode-supported electrolyte depends on the shrinkage rates of the anode and the YSZ electrolyte. In the present research, the result differs from the suggested model because the specimens are prepared by the TLC technique with residual stress among multi-layers. In addition, the tapes also involve diverse organic compounds such as carbon black and binder solution. Because organic compounds of the anode-supported electrolyte are continuously decomposed during burn-out, the proposed models cannot be applied to the samples.

One zirconia setter was placed on the sample to improve the flatness of the burnt-out sample. When the loading of one zirconia setter is 274.4 Pa, the flatness of the sample is greatly improved, to a level of 260 μm/8 cm.

After co-sintering, the laminate narrows to 7.4 cm with a severe warp. The flatness of the laminate is about 1 cm/7.4 cm (see Fig. 6). To observe the warp during co-sintering, a video recorder documented the whole sintering process. The progress of the warp of the anode-supported electrolyte during co-sintering is shown in Fig. 7. The anode of the laminate is in contact with the porous zirconia setter. The sample is placed on the zirconia setter at 25 °C. The shape of the sample does not change until 1150 °C, which is close to the burn-out temperature. The sample then warps continuously until 1350 °C and remains unchanged thereafter. The warping direction

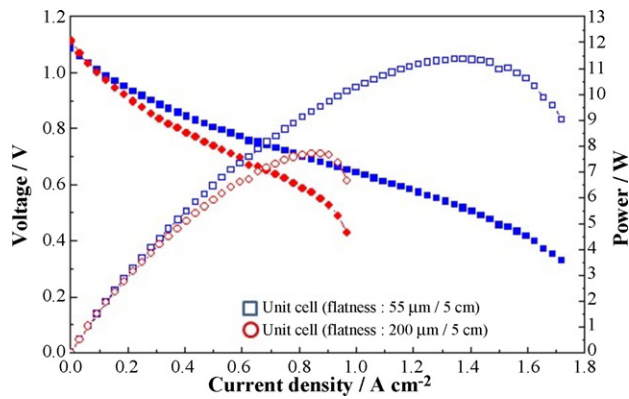


Fig. 10. I - V characteristics of two anode-type supported cells in reactive gases of humidified hydrogen (400 cc min^{-1}) with 3% H_2O and air (600 cc min^{-1}) at 800°C : (a) unit cell showing a reasonable flatness ($55 \mu\text{m}/5 \text{ cm}$), (b) unit cell showing too-warped a contour ($200 \mu\text{m}/5 \text{ cm}$).

is always toward the electrolyte (convex warping); refer to Fig. 6. The shrinkage rates of the anode, AFL and electrolyte are presented in Fig. 8. The samples shrink sharply at temperatures above 1150°C . The shrinkage rate of the anode is larger than that of the electrolyte. The organic compounds are not present in the sample during sintering. In this condition, the warping direction is always toward the electrolyte (convex warping) due to the different shrinkage rates of the anode and the electrolyte.

Severely warped specimens cannot be applied to planar SOFCs systems. During heat-treatment, a specific method for improving the flatness of large-sized unit cells should be developed. A diverse load was pressed onto the sample to determine the dependence of flatness on loading. As shown in Fig. 9, when the loads of 460.6, 597.8, 1107.4 and 1793.4 Pa are set, the flatness of the anode-supported electrolytes is $720 \mu\text{m}/5 \text{ cm}$, $200 \mu\text{m}/5 \text{ cm}$, $62 \mu\text{m}/5 \text{ cm}$, $55 \mu\text{m}/5 \text{ cm}$ and $110 \mu\text{m}/5 \text{ cm}$, respectively. The 1107.4-Pa load improves the flatness to $55 \mu\text{m}/5 \text{ cm}$, which corresponded to about 0.1%.

3.2. Relationship between flatness and performance of the cell

The anode-supported electrolyte created by the TLC technique has proper porosity for an anode and a very uniform and dense microstructure as electrolyte, which can prevent gas crossover [9]. The cathode layer was screen-printed on the $5 \text{ cm} \times 5 \text{ cm}$ anode-supported electrolyte with an active area of $4 \text{ cm} \times 4 \text{ cm}$ and a thickness of $50 \mu\text{m}$. Unit-cell flatness is important to the performance of planar SOFCs because a flatter cell increases the contact area of the current-collectors. Samples with a flatness of $200 \mu\text{m}/5 \text{ cm}$ and $55 \mu\text{m}/5 \text{ cm}$ were selected to confirm the relationship between flatness and cell performance. To enhance the performance of the cell, a NiO/YSZ-YSZ AFL that improves three-phase boundaries (TPBs) was inserted between the anode and the electrolyte [14]. The single-cell performances are measured at 800°C in reactive gases of humidified hydrogen (400 cc min^{-1})

with 3% H_2O and air (600 cc min^{-1}). As shown in Fig. 10, the maximum power and maximum power density of the unit cells having the anode-supported electrolyte of $200 \mu\text{m}/5 \text{ cm}$ are 7.7 W and 481 mW cm^{-2} , respectively; the flattest unit cells yield values of 11.4 W and 713 mW cm^{-2} , respectively. The performance of the flatter unit cell is 50% higher than that of the more warped unit cell. Thus, the maximum power density of a large-size unit cell is very sensitive to the flatness of the unit cell.

4. Conclusion

The tape-casting/lamination/co-firing technique is an appropriate method for the commercialization of planar SOFCs. It is very difficult, however, to control the flatness of large-sized unit cells prepared by the TLC technique because of the different TECs of the multi-layers. The behaviour of the laminate is monitored during heat-treatment. Various loads are applied to the anode-supported electrolytes to study how the flatness of a sample depends on the loading. In particular, an applied pressure of 1107.4 Pa improves the flatness to $55 \mu\text{m}/5 \text{ cm}$. The maximum power and maximum power density of the flattest unit cell are 11.4 W and 713 mW cm^{-2} , respectively, at 800°C .

References

- [1] T.-L. Wen, D. Wang, H.Y. Tu, M. Chen, Z. Lu, Z. Zhang, H. Nie, W. Huang, Research on planar SOFC stack, *Solid State Ionics* 152 (2002) 399–404.
- [2] H.Y. Jung, S.-H. Choi, H. Kim, J.-W. Son, J. Kim, H.-W. Lee, J.-H. Lee, Fabrication and performance evaluation of 3-cell SOFC stack based on planar $10 \text{ cm} \times 10 \text{ cm}$ anode-supported cells, *J. Power Sources* 159 (2006) 478–483.
- [3] H. Ohri, T. Matsushima, T. Hirai, Performance of a solid oxide fuel cell fabricated by co-firing, *J. Power Sources* 71 (1998) 185–189.
- [4] Z. Wanga, K. Sunb, S. Shena, N. Zhangb, J. Qiaoa, P. Xua, Preparation of YSZ thin films for intermediate temperature solid oxide fuel cells by dip-coating method, *J. Membr. Sci.* 320 (2008) 500–504.
- [5] J. Wang, Z. Lu, K. Chena, X. Huanga, N. Aia, J. Hua, Y. Zhang, W. Sua, Study of slurry spin coating technique parameters for the fabrication of anode-supported YSZ Films for SOFCs, *J. Power Sources* 164 (2007) 17–23.
- [6] J. Ding, J. Liu, An anode-supported solid oxide fuel cell with spray-coated yttria-stabilized zirconia (YSZ) electrolyte film, *Solid State Ionics* 179 (2008) 1246–1249.
- [7] W. Sun, X. Huang, Z. Lu, L. Zhao, B. Wei, S. Li, K. Chen, N. Ai, W. Su, NiO+YSZ anode substrate for screen-printing fabrication of YSZ electrolyte film in solid oxide fuel cell, *J. Phys. Chem. Solids* 70 (2009) 164–168.
- [8] W. Lia, K. Hasinska, M. Seabaugh, S. Swartz, J. Lannutti, Curvature in solid oxide fuel cells, *J. Power Sources* 138 (2004) 145–155.
- [9] H. Moon, S.D. Kim, E.W. Park, S.H.H.S.K. Hyun, Characteristics of SOFC single cells with anode active layer via tape casting and co-firing, *Int. J. Hydrogen Energy* 33 (2008) 2826–2833.
- [10] H. Moon, S.D. Kim, S.H. Hyun, H.S. Kim, Development of IT-SOFC unit cells with anode-supported thin electrolytes via tape casting and co-firing, *Int. J. Hydrogen Energy* 33 (2008) 1758–1768.
- [11] S.D. Kim, H. Moon, S.H. Hyun, J. Moon, J. Kim, H.W. Lee, Nano-composite materials for high-performance and durability of solid oxide fuel cells, *J. Power Sources* 163 (2006) 392–397.
- [12] S.H. Lee, G.L. Messing, M. Awano, Sintering arches for cosintering camber camber-free SOFC multilayers, *J. Am. Ceram. Soc.* 91 (2008) 421–427.
- [13] W. Bao, Q. Chang, G. Meng, Effect of NiO/YSZ compositions on the co-sintering process of anode-supported fuel cell, *J. Membr. Sci.* 259 (2005) 103–109.
- [14] S.D. Kim, H. Moon, S.H. Hyun, J. Moon, J. Kim, H.W. Lee, Ni-YSZ cermet anode fabricated from NiO-YSZ composite powder for high-performance and durability of solid oxide fuel cells, *Solid State Ionics* 178 (2007) 1304–1309.